Geochemical Perspectives Letters

The heterogeneous nature of Fe delivery from melting icebergs

M.J. Hopwood[1*], C. Cantoni[2], J.S. Clarke[1], S. Cozzi[2], E.P. Achterberg[1]

OPEN ACCESS

doi: 10.7185/geochemlet.1723

Abstract

The micronutrient iron (Fe) can be transported from marine terminating glaciers to the ocean by icebergs. There are however few observations of iceberg Fe content, and the flux of Fe from icebergs to the offshore surface ocean is poorly constrained. Here we report the dissolved Fe (DFe), total dissolvable Fe (TdFe) and ascorbic acid extractable Fe (FeAsc) sediment content of icebergs from Kongsfjorden, Svalbard. The concentrations of DFe (range 0.63 nM – 536 nM, mean 37 nM, median 6.5 nM) and TdFe (range 46 nM – 57 μM, mean 3.6 μM, median 144 nM) both demonstrated highly heterogeneous distributions and there was no significant correlation between these two fractions. FeAsc (range 0.0042 to 0.12 wt. %) was low compared to both previous measurements in Kongsfjorden and to current estimates of the global mean. FeAsc content per volume ice did however, as expected, show a significant relationship with sediment loading (which ranged from < 0.1 – 234 g L^{-1} of meltwater). In the Arctic, icebergs lose their sediment load faster than ice volume due to the rapid loss of basal ice after calving. We therefore suggest that the loss of basal ice is a potent mechanism for the reduction of mean TdFe and FeAsc per volume of iceberg. Delivery of TdFe and FeAsc to the ocean is thereby biased towards coastal waters where, in Kongsfjorden, DFe (18 ± 17 nM) and TdFe (mean 8.1 μM, median 3.7 μM) concentrations were already elevated.

Received 27 September 2016 | Accepted 25 April 2017 | Published 7 June 2017

Introduction

Icebergs contain higher Fe concentrations than seawater, both in the dissolved (<0.2 μm) (Martin *et al.*, 1990; De Baar *et al.*, 1995; Loscher *et al.*, 1997) and particulate (>0.2 μm) phases (Hart, 1934; Lin *et al.*, 2011; Shaw *et al.*, 2011). Icebergs should thus constitute a source of the micronutrient Fe to offshore polar waters (Raiswell *et al.*, 2008). As the rate of iceberg calving in polar seas oscillates on glacial to inter-glacial timescales (Bond *et al.*, 1992), and recent climate change has

1. GEOMAR, Helmholtz Centre for Ocean Research, 24148 Kiel, Germany
* Corresponding author (email: mhopwood@geomar.de)
2. CNR-ISMAR, Marine Science Institute, 34149 Trieste, Italy

increased the discharge of calved ice volume from both the Antarctic (Paolo *et al.*, 2015) and Greenlandic (Bamber *et al.*, 2012) ice sheets, Fe delivery from icebergs may also change. Particularly in the Southern Ocean, where DFe deficiency extensively limits primary production (Martin *et al.*, 1990, 1991; Moore *et al.*, 2013), and icebergs cause chemical and biological enrichment of surrounding waters (Smith Jr. *et al.*, 2007; Schwarz and Schodlok, 2009; Smith *et al.*, 2011), a change in iceberg Fe supply could significantly affect marine primary productivity. Yet there remain large uncertainties concerning the magnitude of iceberg Fe supply and its effect(s) on marine ecosystems. For example, calculated phytoplankton Fe utilisation is considerably less than present estimates of iceberg Fe supply to the Weddell Sea (Boyd *et al.*, 2012). The reason for this is unclear, yet it demonstrates the difficulty in isolating the contribution of icebergs to the marine Fe cycle.

Observations of DFe concentrations in iceberg meltwater are sparse, but the available data does suggest a heterogeneous distribution, with DFe ranging 4–600 nM in Antarctic (Lin *et al.*, 2011) and 3–300 nM in Greenlandic (Hopwood *et al.*, 2016) iceberg melt. The distribution of particulate Fe (which includes FeAsc) is also expected to be heterogeneous due to the presence of embedded sediment-rich layers that account for only a small fraction of total iceberg volume (Lin *et al.*, 2011; Raiswell, 2011; Raiswell *et al.*, 2016). Whilst TdFe data for icebergs is sparse, iceberg FeAsc content has previously been estimated in multiple catchments worldwide (Raiswell *et al.*, 2016) producing a mean global content of 2.7–17 μM. However, FeAsc content and offshore iceberg FeAsc fluxes are normally calculated using a mean sediment loading (0.5 g L^{-1} is widely used as outlined in Raiswell *et al.* (2016)) with considerable uncertainty generally acknowledged in this value. Here we combine the analysis of DFe, TdFe, FeAsc and iceberg sediment load in order to provide a well constrained assessment of iceberg-Fe content within a single catchment.

Methods

A FeAsc dataset was compiled for icebergs in Kongsfjorden with visible embedded or surface sediment sampled from small boats in July 2015 and August 2016. Sediment from pro-glacial streambeds in the catchment, embedded sediment from Kongsvegen glacier surface, and embedded sediment ~100 m inside an ice crevasse (on Midtre Lovénbreen glacier) was also collected (Fig. 1) for comparative purposes. FeAsc leaches were conducted on wet sediment as per Raiswell *et al.* (2010), with leached Fe determined by measuring absorbance (λ = 562 nm) before and after the addition of ferrozine (as detailed in Supplementary Information Methods).

Separately, ice samples (1–2 kg) were randomly collected from small boats (July 2015). The meltwater was acidified to pH < 2. After storage for 12 months, DFe and TdFe were measured by inductively coupled plasma mass spectroscopy (further details in Supplementary Information Methods).

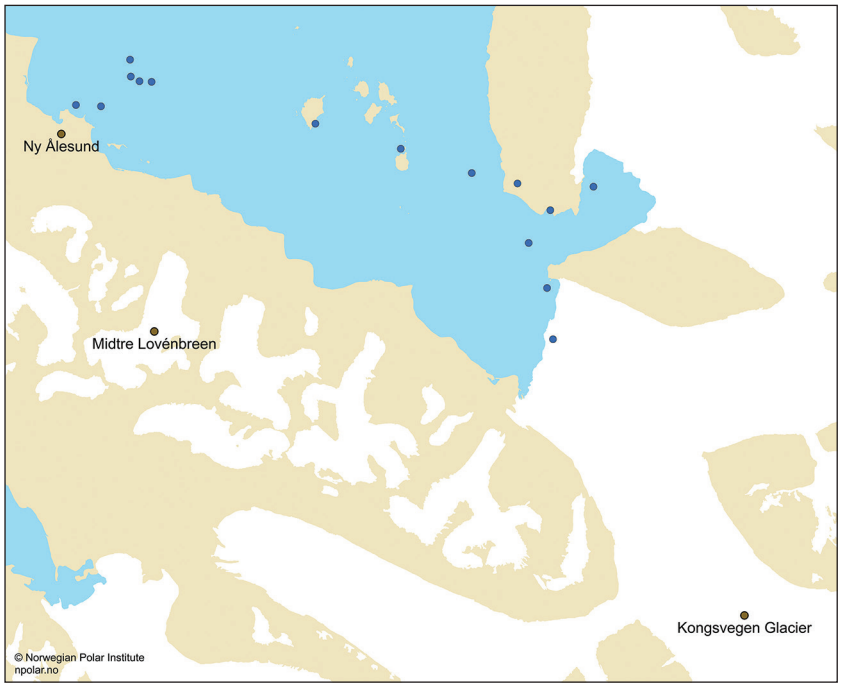

Figure 1 Surface fjord sample locations in Kongsfjorden.

Results

The FeAsc concentration is reported for 116 different sediment samples (Table S-2) including 58 iceberg samples collected from ice with visible embedded sediment. FeAsc ranged from 0.0042 to 0.12 wt. % in iceberg embedded sediment (Fig. 2). Ice sediment content ranged from <0.1 to 234 g L^{-1} of meltwater, close to the 0.2–200 g L^{-1} range previously reported in Svalbard by Dowdeswell and Dowdeswell (1989). Combining FeAsc (wt. %) and sediment load (g L^{-1} of melted ice) produced a median FeAsc ice content of 2.5 μM. Given that our sampling strategy was to target sediment-rich ice, this should thereby be an over-estimate of median iceberg FeAsc content (L^{-1} of melted ice) in Kongsfjorden.

The DFe and TdFe concentrations are reported in parallel for 28 randomly collected iceberg samples (Table S-4). TdFe ranged from 46 nM to 57 μM (mean 3.6 μM, median 144 nM) and the range of 0.63 nM – 536 nM for DFe was similarly broad (mean 37 nM, median 6.5 nM). There was no significant correlation between particulate Fe (TdFe minus DFe) and DFe in these samples (Fig. 3),

suggesting that DFe was not specifically associated with sediment laden ice. For comparison, DFe in surface fjord waters averaged 18 ± 17 nM (15 surface stations, Fig. 1) and TdFe ranged widely from 1.1 to 52 μM (mean 8.1 μM, median 3.7 μM) (Table S-3).

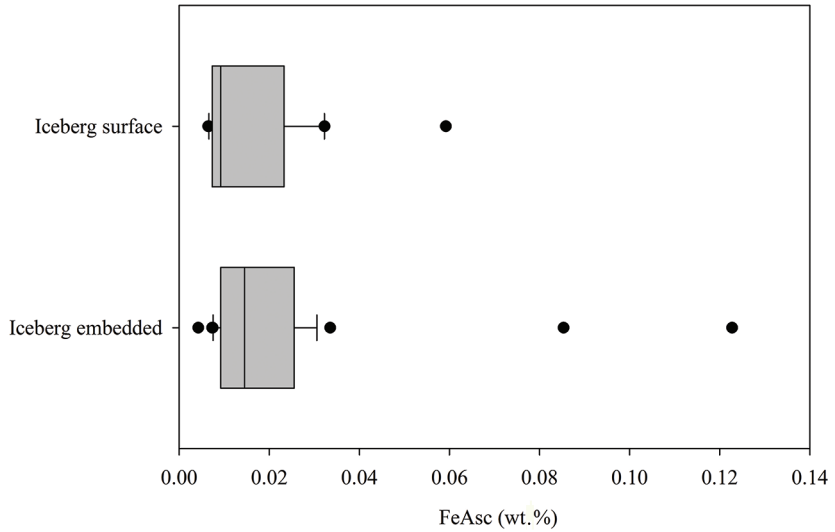

Figure 2 Median FeAsc (wt. %) with 25/75th (boxes) and 10/90th (whiskers) percentiles (outliers also shown) for iceberg embedded (n = 34) and iceberg surface (n = 20) sediment.

Discussion

As has been demonstrated in this study and elsewhere (*e.g.,* Markussen *et al.*, 2016), surface waters in stratified, glaciated fjords can exhibit extremely high TdFe concentrations due to the presence of glacially derived particle plumes. TdFe concentrations in surface waters of Kongsfjorden (mean 8.1 μM, median 3.7 μM) exceeded those in icebergs (3.6 μM and 144 nM, respectively). In the Arctic, a large fraction of iceberg melt occurs in these inshore, high TdFe waters before icebergs are able to deliver Fe to the offshore environment. Accounting for this near-shore loss in flux calculations for iceberg derived Fe supply to the open ocean is difficult. In two Greenlandic catchments, Ilulissat Fjord and Sermilik Fjord, overall in-fjord iceberg volume losses were estimated to be >50 % (Enderlin *et al.*, 2016), tentatively supporting the 50 % inshore iceberg volume loss used to estimate offshore FeAsc fluxes by Raiswell *et al.* (2016). However this assumes that changes in total iceberg Fe content are directly proportional to changes in total ice volume.

All measured Fe phases (DFe, TdFe and FeAsc) in Kongsfjorden were very heterogeneously distributed within the ice. For TdFe and FeAsc (but not DFe, Fig. 3), this can specifically be attributed to the heterogeneous distribution of ice embedded sediment. In the Arctic, iceberg-borne sediment is known to be lost from icebergs faster than ice volume (Mugford and Dowdeswell, 2010) due to its association with basal ice. Thus we expect that the mean TdFe content per volume of an iceberg should decline with time after calving. A model for Kangerdlugssuaq Fjord (Greenland) shows that whilst icebergs lose 20–30 % ice volume within this fjord, the corresponding in-fjord sediment loss is 70–85 % (Mugford and Dowdeswell, 2010). Only a relatively small iceberg volume loss (<20 %) is thereby likely required for the majority of TdFe content to be lost from icebergs. In Kongsfjorden, where summer melting of calved ice is quite rapid due to relatively warm surface seawater (4–5 °C throughout July-August 2016), the post-calving age of an iceberg is therefore likely a critical factor in determining its TdFe content. Sediment loss should also affect mean FeAsc content in the same way, however FeAsc losses may be offset from TdFe losses if significant processing of surface sediment occurs on the timescale of iceberg Fe delivery (Raiswell *et al.*, 2016).

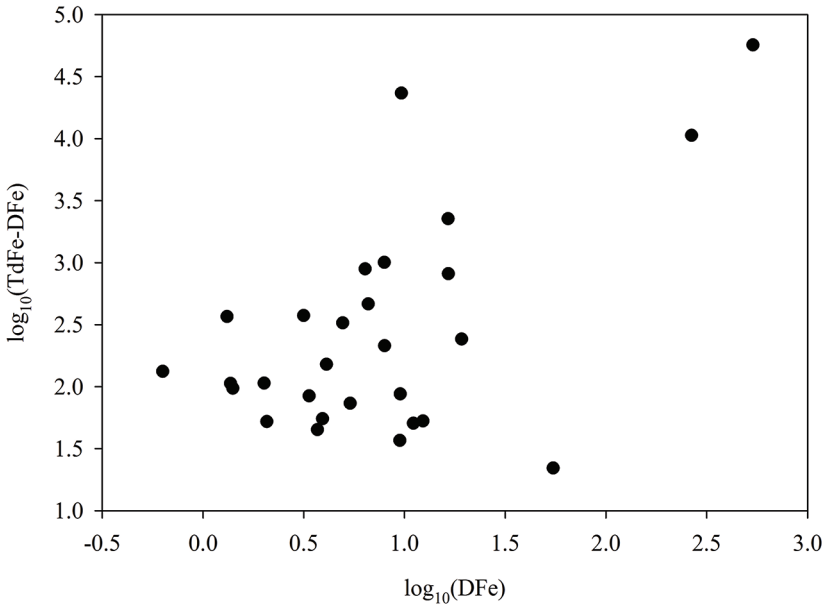

Figure 3 DFe and TdFe (both nM, plotted as $\log_{10}$, TdFe shown minus DFe) for 28 discrete iceberg samples showed no clear relationship.

In Kongsfjorden, Raiswell *et al.* (2016) reported a FeAsc range of 0.016–0.37 wt. % (n = 14), with a mean of 0.14 wt. % and median of 0.092 wt. %; equivalent to 1.4–33 μM, 12 μM and 8.2 μM, respectively when using the suggested mean sediment loading of 0.5 g L^{-1}. Comparing our data both as wt. % and as a μM concentration (calculated using measured sediment loading for each sample, range 0.1–234 g L^{-1}, Table S-2), our FeAsc (wt. %) is consistently lower. Yet our mean FeAsc per volume is much higher (51 μM), because our measured sediment loadings were often greater than the assumed mean of 0.5 g L^{-1}. These differences generally highlight the very high spatial variability in iceberg sediment load and thus TdFe and FeAsc content even within a single fjord.

Table 1 Comparing data for Kongsfjorden from this study and prior work suggests a critical difference in both FeAsc (wt. %) and in the scaling of FeAsc to iceberg sediment load (g L^{-1} of ice melt). *The suggested 0.5 g L^{-1} sediment loading is used for data from Raiswell *et al.* (2016). ** For our study, measured sediment loadings were used for each sample. As sediment-rich ice was specifically targeted, the calculated mean/median should be over-estimates.

		a This study	b Raiswell *et al.* (2016)	a/b %
FeAsc / wt. %	Mean	0.021	0.14	16
	Median	0.015	0.092	17
FeAsc / μM (per litre of ice melt)*	Mean	<59 **	12	480
	Median	<2.5 **	8.2	31

Some methodological differences between this study and previous work could be important for the difference in FeAsc (wt. %) (Table 1). In our study, the sediment was not sieved to remove anomalous large particles. Yet a relatively large sub-sample mass was used with good reproducibility demonstrated. For glacial flour particles of <1 mm, it has previously been demonstrated that the change in FeAsc (wt. %) with particle size is not pronounced (Hopwood *et al.*, 2014; Raiswell *et al.*, 2016), but this may not be the case for larger particles. Moreover, in this study sediment was processed in Svalbard with no prolonged storage between collection and analysis. Whilst dried sediment exhibits a rapid decline in FeAsc wt. % (Raiswell *et al.*, 2010), it is not clear how storage of ice or wet sediments affects FeAsc.

Furthermore, there are the critical issues of heterogeneity and of the non-linearity between iceberg sediment and iceberg volume losses. In-fjord iceberg volume loss should correspond to a disproportionately high loss of iceberg embedded sediment (Mugford and Dowdeswell, 2010), and thereby also FeAsc and TdFe. There are no quantitative measures of iceberg age or volume loss for our dataset and the residence time of ice in Kongsfjorden is strongly affected by meteorological conditions and thus subject to high short-term variability. Nonetheless, a difference in the post-calving age of ice sampled between different datasets could correspond to large shifts in iceberg FeAsc and TdFe content. Increased iceberg age would be expected to correspond to lower mean sediment load, and thereby lower TdFe and FeAsc per volume. A reduction in basal

sediment load could also explain a difference in FeAsc (wt. %) content if FeAsc (wt. %) is enriched in basal ice compared to non-basal ice. FeAsc (μmol L^{-1}) is correlated with sediment load (Fig. 4), but assessing whether changes in sediment load affect FeAsc (wt. %) is complicated by the lack of any parameter to account for the post-calving age of ice and by the highly variable bedrock composition across Kongsfjorden (see for example Hjelle, 1993).

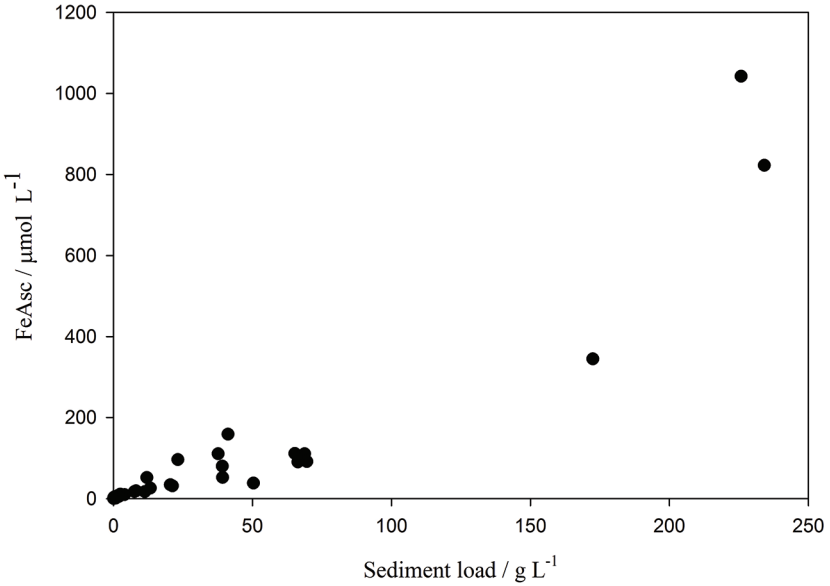

Figure 4 FeAsc (μmol L^{-1} melted ice) increased with sediment load (g L^{-1} melted ice), but it is unclear if the relationship remains linear at high (>50 g L^{-1}) loadings.

Conclusions

Whilst median DFe (6.5 nM) and TdFe (144 nM) concentrations in Kongsfjorden were within the range of concentrations reported elsewhere globally, the median FeAsc concentration (2.5 μM) measured was considerably lower than that reported previously in Kongsfjorden, and compared to present estimates of the global mean, despite the very high sediment loadings observed (<0.1 – 234 g L^{-1}). Generally in the Arctic, a sharp decline in the mean FeAsc and TdFe per volume of meltwater from icebergs with time after calving would be expected due to the preferential loss of iceberg basal ice, as modelled by Mugford and Dowdeswell (2010). Iceberg derived fluxes of TdFe and FeAsc are thereby biased towards delivery in near-shore waters and offshore fluxes are likely much less than if TdFe and FeAsc were homogeneously distributed throughout icebergs.

Glossary

'Fe' refers to all iron phases.

'DFe', dissolved Fe, refers to all Fe phases <0.2 μm.

'FeAsc' is the ferrihydrite content of sediment, defined by Raiswell *et al.* (2010).

'TdFe' is all Fe soluble at pH < 2, inclusive of DFe and should also include any FeAsc present in unfiltered meltwater.

Acknowledgements

Financial aid from the European Commission (OCEAN-CERTAIN, FP7-ENV-2013-6.1-1; no: 603773) is gratefully acknowledged. 2016 fieldwork was conducted during the CNR Dirigibilite Italia hosted project 'pH in Svalbard'.

Editor: Liane G. Benning

Additional Information

Supplementary Information accompanies this letter at www.geochemicalperspectivesletters.org/article1723

Cite this letter as: Hopwood, M.J., Cantoni, C., Clarke, J.S., Cozzi, S., Achterberg, E.P. (2017) The heterogeneous nature of Fe delivery from melting icebergs. *Geochem. Persp. Let.* 3, 200–209.

References

Bamber, J., van den Broeke, M., Ettema, J., Lenaerts, J., Rignot, E. (2012) Recent large increases in freshwater fluxes from Greenland into the North Atlantic. *Geophysical Research Letters* 39, L19501, doi:10.1029/2012gl052552.

Bond, G., Heinrich, H., Broecker, W.S., Labeyrie, L., McManus, J.F., Andrews, J.T., Huon, S., Jantschik, R., Clasen, S., Simet, C., Tedesco, K., Klas, M., Bonani, G., Ivy, S. (1992) Evidence for massive discharges of icebergs into the North Atlantic ocean during the last glacial period, *Nature* 360, 245–249.

Boyd, P.W., Arrigo, K.R., Strzepek, R., Van Dijken, G.L. (2012) Mapping phytoplankton iron utilization: Insights into Southern Ocean supply mechanisms. *Journal Geophysical Research: Oceans* 117, doi:10.1029/2011JC007726.

De Baar, H.J.W., De Jong, J.T.M., Bakker, D.C.E., Loscher, B.M., Veth, C., Bathmann, U., Smetacek, V. (1995) Importance of iron for plankton blooms and carbon dioxide drawdown in the Southern Ocean. *Nature* 373, 412–415.

Dowdeswell, J.A., Dowdeswell, E.K. (1989) Debris in Icebergs and Rates of Glaci-Marine Sedimentation: Observations from Spitsbergen and a Simple Model. *The Journal of Geology* 97, 221–231.

Enderlin, E.M., Hamilton, G.S., Straneo, F., Sutherland, D.A. (2016) Iceberg meltwater fluxes dominate the freshwater budget in Greenland's iceberg-congested glacial fjords. *Geophysical Research Letters* 43, 11287–11294.

Hart, T.J. (1934) Discovery Reports. *Discovery Reports* 8, 1–268.

Hjelle, A. (1993) *The geology of Svalbard: Oslo. Polarhåndbok nr. 6.* Norsk Polarinstitutt, Oslo.

Hopwood, M.J., Statham, P.J., Tranter, M., Wadham, J.L. (2014) Glacial flours as a potential source of Fe(II) and Fe(III) to polar waters. *Biogeochemistry* 118, 443–452.

Hopwood, M.J., Connelly, D.P., Arendt, K.E., Juul-Pedersen, T., Stinchcombe, M., Meire, L., Esposito, M., Krishna, R. (2016) Seasonal changes in Fe along a glaciated Greenlandic fjord. *Frontiers in Earth Sciences* 4, doi:10.3389/feart.2016.00015.

Lin, H., Rauschenberg, S., Hexel, C.R., Shaw, T.J., Twining, B.S. (2011) Free-drifting icebergs as sources of iron to the Weddell Sea. *Deep Sea Research Part II: Topical Studies in Oceanography* 58, 1392–1406.

Loscher, B.M., De Baar, H.J.W., De Jong, J.T.M., Veth, C., Dehairs, F. (1997) The distribution of Fe in the Antarctic Circumpolar Current. *Deep Sea Research Part II: Topical Studies in Oceanography* 44, 143–187.

Markussen, T.N., Elberling, B., Winter, C., Andersen, T.J. (2016) Flocculated meltwater particles control Arctic land-sea fluxes of labile iron. *Scientific Reports* 6, 24033.

Martin, J.H., Gordon, R.M., Fitzwater, S.E. (1990) Iron in Antarctic waters. *Nature* 345, 156–158.

Martin, J.H., Gordon, R.M., Fitzwater, S.E. (1991) The case for iron. *Limnology and Oceanography* 36, 1793–1802.

Moore, C.M., Mills, M.M., Arrigo, K.R., Berman-Frank, I., Bopp, L., Boyd, P.W., Galbraith, E.D., Geider, R.J., Guieu, C., Jaccard, S.L., Jickells, T.D., La Roche, J., Lenton, T.M., Mahowald, N.M., Maranon, E., Marinov, I., Moore, J.K., Nakatsuka, T., Oschlies, A., Saito, M.A., Thingstad, T.F., Tsuda, A., Ulloa, O. (2013) Processes and patterns of oceanic nutrient limitation. *Nature Geoscience* 6, 701–710.

Mugford, R.I., Dowdeswell, J.A. (2010) Modeling iceberg-rafted sedimentation in high-latitude fjord environments. *Journal of Geophysical Research: Earth Surface* 115, doi:10.1029/2009JF001564.

Paolo, F.S., Fricker, H.A., Padman, L. (2015) Volume loss from Antarctic ice shelves is accelerating. *Science* 348, 327–331.

Raiswell, R. (2011) Iceberg-hosted nanoparticulate Fe in the Southern Ocean: Mineralogy, origin, dissolution kinetics and source of bioavailable Fe. *Deep Sea Research Part II: Topical Studies in Oceanography* 58, 1364–1375.

Raiswell, R., Benning, L.G., Tranter, M., Tulaczyk, S. (2008) Bioavailable iron in the Southern Ocean: the significance of the iceberg conveyor belt. *Geochemical Transactions* 9, doi:10.1186/1467-4866-9-7.

Raiswell, R., Vu, H.P., Brinza, L., Benning, L.G. (2010) The determination of labile Fe in ferrihydrite by ascorbic acid extraction: Methodology, dissolution kinetics and loss of solubility with age and de-watering. *Chemical Geology* 278, 70–79.

Raiswell, R., Hawkings, J.R., Benning, L.G., Baker, A.R., Death, R., Albani, S., Mahowald, N., Krom, M.D., Poulton, S.W., Wadham, J., Tranter, M. (2016) Potentially bioavailable iron delivery by iceberg-hosted sediments and atmospheric dust to the polar oceans. *Biogeosciences* 13, 3887–3900.

Schwarz, J.N., Schodlok, M.P. (2009) Impact of drifting icebergs on surface phytoplankton biomass in the Southern Ocean: Ocean colour remote sensing and in situ iceberg tracking. *Deep Sea Research Part I: Oceanographic Research Papers* 56, 1727–1741.

Shaw, T.J., Raiswell, R., Hexel, C.R., Vu, H.P., Moore, W.S., Dudgeon, R., Smith Jr., K.L. (2011) Input, composition, and potential impact of terrigenous material from free-drifting icebergs in the Weddell Sea. *Deep Sea Research Part II: Topical Studies in Oceanography* 58, 1376–1383.

Smith, K.L., Sherman, A.D., Shaw, T.J., Murray, A.E., Vernet, M., Cefarelli, A.O. (2011) Carbon export associated with free-drifting icebergs in the Southern Ocean. *Deep Sea Research Part II: Topical Studies in Oceanography* 58, 1485–1496.

Smith Jr., K.L., Robison, B.H., Helly, J.J., Kaufmann, R.S., Ruhl, H.A., Shaw, T.J., Twining, B.S., Vernet, M. (2007) Free-drifting icebergs: Hot spots of chemical and biological enrichment in the Weddell Sea. *Science* 317, 478–482.

The heterogeneous nature of Fe delivery from melting icebergs

M.J. Hopwood[1*], C. Cantoni[2], J.S. Clarke[1], S. Cozzi[2], E.P. Achterberg[1]

Supplementary Information

The Supplementary Information includes:

- Supplementary Methods
- Supplementary Material
- Supplementary Information References
- Tables S-1 to S-4

Supplementary Methods

Ice sample collection

All ice samples were collected from calved ice masses within Kongsfjorden east of 11.89° E. Sampled icebergs had a maximum length (visible above the waterline) of between 0.4 and 20 m, and a maximum height above the waterline of between 10 cm and 4 m. For FeAsc, icebergs with visible sediment layers (darkened layers approximately 0.5 to 5 cm thick) were targeted whereas sample collection for DFe/TdFe was random.

FeAsc

To measure FeAsc, 1–2 kg ice pieces were returned to the laboratory in insulated plastic boxes. As a precaution against contamination, ice was rinsed with de-ionised water (Milli-Q, Millipore, conductivity 18.2 MΩ cm^{-1}). Ice was then melted in low density polyethylene (LDPE) bags with the first (1–2 hr later) meltwater discarded. After melting ice overnight, the total volume was recorded and

1. GEOMAR, Helmholtz Centre for Ocean Research, 24148 Kiel, Germany
* Corresponding author (email: mhopwood@geomar.de)
2. CNR-ISMAR, Marine Science Institute, 34149 Trieste, Italy

then excess water was removed slowly (<5 mL min^{-1}) by filtration (0.45 μm, polyvinylidene fluoride, Millipore) to concentrate the sediment. All plastic vials and filtration equipment for sediment collection/handling was pre-cleaned (1 M HCl, 3 de-ionised water rinses) prior to use. FeAsc was determined as per Raiswell *et al.* (2010) but using larger (~100 mg) sediment samples without sieving. Leached Fe was determined by measuring absorbance (λ = 562 nm) before, and after, the addition of ferrozine (Stookey, 1970) using a 1 cm cell with a USB4000 Fiber-optic Spectrometer and a LS-1 tungsten halogen light source (Ocean Optics). Fe standards were made by spiking DFe from an acidified (pH 2) 1 mM Fe stock solution into aliquots of ascorbic leaching solution producing a linear response ($R^2 > 0.99$, derived molar adsorption coefficient 24,500 M^{-1} cm^{-1}) over the absorbance range 0–0.6. Sample absorbance was then corrected for background absorbance and dilution by reagents.

A sub-sample of sediment was retained (except for sediment loadings <0.1 g L^{-1} where this was not possible) and air dried to constant mass in order to calculate FeAsc content g^{-1} (of sediment) and L^{-1} (of meltwater). FeAsc measurements were duplicated for 11 randomly selected samples producing a relative standard deviation of 4.5 %. The propagated standard deviation for FeAsc L^{-1} of meltwater (obtained from combining sediment load with FeAsc wt. %) was approximately 15 %.

DFe and TdFe

125 mL LDPE bottles (Nalgene) were pre-cleaned in a 3 stage process with 3 de-ionised water rinses after each stage (detergent, 1.2 M HCl, 1.2 M HNO_3). After melting ice in LDPE bags, as above, 125 mL meltwater was retained without filtration for TdFe, and 125 mL was syringe filtered for DFe analysis (0.20 μm, polyvinylidene fluoride, Millipore). TdFe and DFe samples were acidified (with HCl, UPA, ROMIL) to pH < 2.0 and subsequently stored for 12 months to ensure complete recovery of soluble Fe (Edwards and Sedwick, 2001). DFe and TdFe were analysed by ICP-MS (ELEMENT XR, ThermoFisherScientific) after dilution with 1 M HNO_3 (distilled in house using a DST-1000, Savillex, from SPA grade HNO_3, ROMIL) and calibrated by standard addition with a linear peak response from 0–1000 nM Fe ($R^2 > 0.99$). The analytical blank (DFe and TdFe) was always <0.6 nM Fe. To verify that the dilution technique yielded reproducible and accurate DFe results, NASS-7 and CASS-6 Certified Reference Materials (CRMs, National Research Council Canada) were analysed for Fe. Both CRMs yielded reproducible Fe concentrations within the certified ranges (Table S-1).

Table S-1 Analysis of Certified Reference Materials for Fe concentration (± standard deviation of at least 6 measurements).

Certified Reference Material	Fe (±SD) / nM	Certified Fe concentration / nM
NASS-7	6.21 (±0.77)	6.29 (±0.47)
CASS-6	26.6 (±0.71)	27.9 (±2.1)

A linear plot of all paired DFe and TdFe minus DFe (n = 28) yielded R^2 = 0.78. However, R^2 declined to 0.01 when the 3 highest TdFe data were removed. A Spearman Rank Order Correlation suggested there was no significant relationship between DFe and TdFe minus DFe (P value 0.21). A linear plot of all FeAsc (mol L^{-1}) data and corresponding ice sediment load (g L^{-1}) yielded R^2 = 0.88. A Spearman Rank Order Correlation Coefficient of 0.95 (P value 2×10^{-7}, n = 58) demonstrates that the relationship is significant and remains significant if the 3 highest sediment loadings are removed (Coefficient 0.94, P value 2×10^{-7}, n = 55) – regardless of whether the sediment loads reported as <0.1 g L^{-1} are treated as 0.1 g L^{-1}, 0.01 g L^{-1}, or excluded. Statistics were performed in SigmaPlot 13.

Water column

In July 2015, 15 samples of fjord surface water (depth <0.2 m) were collected by hand upstream of a small boat (locations shown Fig. 1). As per ice samples for DFe and TdFe, 125 mL was retained without filtration and 125 mL was syringe filtered for DFe analysis (0.20 µm, polyvinylidene fluoride, Millipore). Analysis was conducted via ICP-MS after storage for 12 months at pH < 2, and dilution with 1 M HNO_3 (as per melted ice, above). The temperature and salinity of surface fjord water were recorded using a LF 325 conductivity meter (WTW) which was calibrated before use with a KCl solution.

In July–August 2016 conductivity, temperature, depth profiles (CTDs) were acquired at 20 stations in the area of the fjord where ice was observed and collected (east of 11.89° E and proceeding to within approximately 400 m of each marine terminating glacier in Kongsfjorden, Fig. 1). Seawater temperature (recorded at 1 m depth) was consistently 4.0–5.0 °C. A broader range of surface temperatures were observed in July 2015 (2.6–8.8 °C at <0.2 m), but are not directly comparable because of the depth difference.

Supplementary Material

Table S-2 FeAsc concentration reported for various sediment samples collected around Kongsfjorden. For iceberg embedded sediment with sediment loadings >0.1 g L^{-1}, FeAsc is reported both as wt. % and per volume of meltwater.

Sample number	Origin	FeAsc wt. %	*FeAsc µmol / L	*Sediment loading g / L
1	Embedded sediment, glacier crevasse (Midtre Lovénbreen)	0.014		
2	Embedded sediment, glacier crevasse (Midtre Lovénbreen)	0.0057		
3	Embedded sediment, glacier crevasse (Midtre Lovénbreen)	0.17		
4	Embedded sediment, glacier crevasse (Midtre Lovénbreen)	0.023		
5	Embedded sediment, glacier crevasse (Midtre Lovénbreen)	0.0038		
6	Embedded sediment, glacier crevasse (Midtre Lovénbreen)	0.053		
7	Glacier surface sediment (Kongsvegen)	0.016		
8	Glacier surface sediment (Kongsvegen)	0.016		
9	Glacier surface sediment (Kongsvegen)	0.012		
10	Glacier surface sediment (Kongsvegen)	0.010		
11	Glacier surface sediment (Kongsvegen)	0.016		
12	Glacier surface sediment (Kongsvegen)	0.012		
13	Glacier surface sediment (Kongsvegen)	0.014		
14	Iceberg embedded sediment	0.009	110	69
15	Iceberg embedded sediment	0.0093	34	20
16	Iceberg embedded sediment	0.0076	90	66
17	Iceberg embedded sediment	0.0074	52	39
18	Iceberg embedded sediment	0.0085	17	11
19	Iceberg embedded sediment	0.016	2.5	0.91
20	Iceberg embedded sediment	0.0089	1.2	0.76
21	Iceberg embedded sediment	0.085	3.9	0.25
22	Iceberg embedded sediment	0.014	9.6	3.9
23	Iceberg embedded sediment	0.020	820	230
24	Iceberg embedded sediment	0.034	3.9	0.65
25	Iceberg embedded sediment	0.011	26	13
26	Iceberg embedded sediment	0.026	1000	230
27	Iceberg embedded sediment	0.023	96	23
28	Iceberg embedded sediment	0.0042	38	50
29	Iceberg embedded sediment	0.022	160	41
30	Iceberg embedded sediment	0.016	110	38
31	Iceberg embedded sediment	0.0082	31	21
32	Iceberg embedded sediment	0.024	52	12
33	Iceberg embedded sediment	0.0095	110	65
34	Iceberg embedded sediment	0.0073	91	70
35	Iceberg embedded sediment	0.015	5.0	1.8
36	Iceberg embedded sediment	0.013	17	7.5
37	Iceberg embedded sediment	0.011	340	170
38	Iceberg embedded sediment	0.027	7.8	1.6
39	Iceberg embedded sediment	0.026	1.2	0.25

Table S-2 Cont.

Sample number	Origin	FeAsc wt. %	*FeAsc µmol / L	*Sediment loading g / L
40	Iceberg embedded sediment	0.025	11	2.4
41	Iceberg embedded sediment	0.12	3.0	0.14
42	Iceberg embedded sediment	0.028	2.5	0.51
43	Iceberg embedded sediment	0.013	19	8.1
44	Iceberg embedded sediment	0.011	80	39
45	Iceberg embedded sediment	0.020	3.6	0.99
46	Iceberg embedded sediment	0.026	1.2	0.26
47	Iceberg embedded sediment	0.012	2.1	1.0
48	Iceberg embedded sediment	n/d	0.26	< 0.1
49	Iceberg embedded sediment	n/d	0.26	< 0.1
50	Iceberg embedded sediment	n/d	0.87	< 0.1
51	Iceberg embedded sediment	n/d	0.65	< 0.1
52	Iceberg embedded sediment	n/d	0.27	< 0.1
53	Iceberg embedded sediment	n/d	0.50	< 0.1
54	Iceberg embedded sediment	n/d	0.28	< 0.1
55	Iceberg embedded sediment	n/d	0.63	< 0.1
56	Iceberg embedded sediment	n/d	0.40	< 0.1
57	Iceberg embedded sediment	n/d	0.69	< 0.1
58	Iceberg embedded sediment	n/d	0.37	< 0.1
59	Iceberg embedded sediment	n/d	0.43	< 0.1
60	Iceberg embedded sediment	n/d	0.68	< 0.1
61	Iceberg embedded sediment	n/d	0.87	< 0.1
62	Iceberg embedded sediment	n/d	0.27	< 0.1
63	Iceberg embedded sediment	n/d	0.39	< 0.1
64	Iceberg embedded sediment	n/d	1.8	< 0.1
65	Iceberg embedded sediment	n/d	0.40	< 0.1
66	Iceberg embedded sediment	n/d	0.77	< 0.1
67	Iceberg embedded sediment	n/d	0.35	< 0.1
68	Iceberg embedded sediment	n/d	0.29	< 0.1
69	Iceberg embedded sediment	n/d	0.32	< 0.1
70	Iceberg embedded sediment	n/d	0.20	< 0.1
71	Iceberg embedded sediment	n/d	0.15	< 0.1
72	Iceberg surface sediment	0.0065		
73	Iceberg surface sediment	0.0068		
74	Iceberg surface sediment	0.0091		
75	Iceberg surface sediment	0.0072		
76	Iceberg surface sediment	0.024		
77	Iceberg surface sediment	0.0071		
78	Iceberg surface sediment	0.032		
79	Iceberg surface sediment	0.010		
80	Iceberg surface sediment	0.012		
81	Iceberg surface sediment	0.021		

Sample number	Origin	FeAsc wt. %	*FeAsc µmol / L	*Sediment loading g / L
82	Iceberg surface sediment	0.0093		
83	Iceberg surface sediment	0.0077		
84	Iceberg surface sediment	0.059		
85	Iceberg surface sediment	0.0066		
86	Iceberg surface sediment	0.0080		
87	Iceberg surface sediment	0.0080		
88	Iceberg surface sediment	0.029		
89	Iceberg surface sediment	0.032		
90	Iceberg surface sediment	0.0087		
91	Iceberg surface sediment	0.0098		
92	Pro-glacial stream, glacial flour	0.0090		
93	Pro-glacial stream, glacial flour	0.0083		
94	Pro-glacial stream, glacial flour	0.0063		
95	Pro-glacial stream, glacial flour	0.0079		
96	Pro-glacial stream, glacial flour	0.0072		
97	Pro-glacial stream, glacial flour	0.0070		
98	Pro-glacial stream, glacial flour	0.0073		
99	Pro-glacial stream, glacial flour	0.019		
100	Pro-glacial stream, glacial flour	0.031		
101	Pro-glacial stream, glacial flour	0.010		
102	Pro-glacial stream, glacial flour	0.0078		
103	Pro-glacial stream, glacial flour	0.010		
104	Pro-glacial stream, glacial flour	0.0066		
105	Pro-glacial stream, glacial flour	0.0089		
106	Pro-glacial stream, glacial flour	0.0096		
107	Pro-glacial stream, glacial flour	0.0041		
108	Pro-glacial stream, glacial flour	0.0032		
109	Pro-glacial stream, glacial flour	0.0057		
110	Pro-glacial stream, glacial flour	0.0079		
111	Surface glacier (Kongsvegen) embedded sediment	0.044		
112	Surface glacier (Kongsvegen) embedded sediment	0.071		
113	Surface glacier (Kongsvegen) embedded sediment	0.037		
114	Surface glacier (Kongsvegen) embedded sediment	0.011		
115	Surface glacier (Kongsvegen) embedded sediment	0.061		
116	Surface glacier (Kongsvegen) embedded sediment	0.11		

* Iceberg embedded sediment only
n/d not determined as dry mass insufficient (< 0.1 g)

Table S-3 Dissolved (<0.2 μm) Fe and total dissolvable Fe for 15 surface water samples collected in Kongsfjorden (July 2015).

Name	DFe / nM	TFe / nM	Temperature / °C	Latitude °N	Longitude °E	Salinity
F1	28.5	7226	8.4	78.938	11.992	20.0
F2	9.5	1548	7.0	78.937	12.003	32.1
F3	19.6	1806	6.7	78.942	11.990	31.7
F4	6.6	12444	8.2	78.937	12.018	14.2
F5	19.7	1175	7.5	78.931	11.957	31.7
F6	47.1	5463	8.8	78.928	11.926	22.6
F7	15.5	52495	2.6	78.880	12.528	26.9
F8	10.3	4492	3.7	78.893	12.518	28.1
F9	4.6	3425	4.1	78.903	12.493	28.6
F10	4.5	5126	4.9	78.911	12.518	23.1
F11	60.1	15558	4.8	78.917	12.570	23.1
F12	6.8	3408	4.8	78.917	12.476	26.7
F13	27.8	3691	5.0	78.919	12.419	27.6
F14	6.9	2600	4.6	78.924	12.330	29.8
F15	5.6	1605	5.4	78.929	12.223	29.7

Table S-4 Dissolved (<0.2 μm) Fe and total dissolvable Fe for 28 randomly collected Kongsfjorden iceberg samples (July 2015).

Sample label	Origin	Catchment	DFe / nM	TdFe / nM	PFe (TdFe-DFe) /nM
Ice 1	Ny Alesund, Svalbard, Summer 2015	Kongsfjorden	19.2	261	242
Ice 2	Ny Alesund, Svalbard, Summer 2015	Kongsfjorden	9.5	97	87
Ice 3	Ny Alesund, Svalbard, Summer 2015	Kongsfjorden	1.3	369	367
Ice 4	Ny Alesund, Svalbard, Summer 2015	Kongsfjorden	7.9	1013	1005
Ice 5	Ny Alesund, Svalbard, Summer 2015	Kongsfjorden	4.9	331	326
Ice 6	Ny Alesund, Svalbard, Summer 2015	Kongsfjorden	0.6	133	133
Ice 7	Ny Alesund, Svalbard, Summer 2015	Kongsfjorden	3.2	377	374
Ice 8	Ny Alesund, Svalbard, Summer 2015	Kongsfjorden	2.0	109	107
Ice 9	Ny Alesund, Svalbard, Summer 2015	Kongsfjorden	2.1	54	52
Ice 10	Ny Alesund, Svalbard, Summer 2015	Kongsfjorden	6.4	897	890

Sample label	Origin	Catchment	DFe / nM	TdFe / nM	PFe (TdFe-DFe) /nM
Ice 11	Ny Alesund, Svalbard, Summer 2015	Kongsfjorden	16.5	2274	2257
Ice 12	Ny Alesund, Svalbard, Summer 2015	Kongsfjorden	6.6	470	464
Ice 13	Ny Alesund, Svalbard, Summer 2015	Kongsfjorden	9.7	23259	23250
Ice 14	Ny Alesund, Svalbard, Summer 2015	Kongsfjorden	8.8	221	213
Ice 15	Ny Alesund, Svalbard, Summer 2015	Kongsfjorden	3.7	49	45
Ice 16	Ny Alesund, Svalbard, Summer 2015	Kongsfjorden	3.9	59	55
Ice 17	Ny Alesund, Svalbard, Summer 2015	Kongsfjorden	11.1	62	51
Ice 18	Ny Alesund, Svalbard, Summer 2015	Kongsfjorden	9.5	46	37
Ice 19	Ny Alesund, Svalbard, Summer 2015	Kongsfjorden	12.4	65	53
Ice 20	Ny Alesund, Svalbard, Summer 2015	Kongsfjorden	5.4	79	73
Ice 21	Ny Alesund, Svalbard, Summer 2015	Kongsfjorden	536.3	57401	56864
Ice 22	Ny Alesund, Svalbard, Summer 2015	Kongsfjorden	54.7	77	22
Ice 23	Ny Alesund, Svalbard, Summer 2015	Kongsfjorden	4.1	156	151
Ice 24	Ny Alesund, Svalbard, Summer 2015	Kongsfjorden	1.4	99	97
Ice 25	Ny Alesund, Svalbard, Summer 2015	Kongsfjorden	1.4	107	106
Ice 26	Ny Alesund, Svalbard, Summer 2015	Kongsfjorden	3.4	88	84
Ice 27	Ny Alesund, Svalbard, Summer 2015	Kongsfjorden	16.5	830	814
Ice 28	Ny Alesund, Svalbard, Summer 2015	Kongsfjorden	266.1	10876	10610

Supplementary Information References

EDWARDS, R., SEDWICK, P. (2001) Iron in East Antarctic snow: Implications for atmospheric iron deposition and algal production in Antarctic waters. *Geophysical Research Letters* 28, 3907–3910.

RAISWELL, R., VU, H.P., BRINZA, L., BENNING, L.G. (2010) The determination of labile Fe in ferrihydrite by ascorbic acid extraction: Methodology, dissolution kinetics and loss of solubility with age and de-watering. *Chemical Geology* 278, 70–79.

STOOKEY, L.L. (1970) Ferrozine- a new spectrophotometric reagent for iron. *Analytical Chemistry* 42, 779–781.